

## AN EVALUATION OF THE BFD CURVE BASED UPON WOOD CRIB FIRES PERFORMED IN AN ISO9705 ROOM

by

**Qiang XU<sup>a</sup>, Gregory J. GRIFFIN<sup>b</sup>, Yong JIANG<sup>c\*</sup>, and Cong JIN<sup>a</sup>**

<sup>a</sup>School of Mechanical, Nanjing University of Science and Technology, Nanjing, China

<sup>b</sup>Fire Science and Technology Laboratory, CSIRO, Manufacturing and Materials Technology,  
Highett, Victoria, Australia

<sup>c</sup>State Key Laboratory of Fire Science, University of Science and Technology of China, Hefei, China

Original scientific paper  
UDC: 536.46:699.81  
DOI: 10.2298.TSCI1002521X

*The BFD curve fitting method of Barnett is adopted to study the compartment temperature-time curves for a series of wood crib fires in an ISO 9705 room. The nominal fire sizes were 0.15 MW, 0.25 MW, 0.5 MW, and 1.0 MW. The cribs were positioned at the corner or the center of the floor of the room. The temperatures within the compartment were measured using two thermocouple trees with 10 thermocouples on each tree; these measured the compartment temperature from floor to ceiling. No flashover occurred during the tests, and the compartment temperature can be well described by a two-zone model. BFD curve fitting was performed for all 20 temperature-time curves in the upper and lower zones of the compartment for each test. The fitting error is evaluated for all tests. This empirical model needs more tests to verify and optimize.*

Key words: *compartment temperature, wood crib fire, ISO 9705 room, BFD curve*

### Introduction

The ability to predict temperatures developed in compartment fires is of great significance to the fire protection professional [1]. There are many uses for knowledge of compartment fire temperatures, including the prediction of: (1) onset of hazardous conditions, (2) property and structural damage, (3) changes in burning rate, (4) ignition of objects, and (5) the onset of flashover. Many methods have been developed to predict or model the compartment temperature during fire. Barnett [2] developed a single log-normal equation (BFD curve) as a new empirical model for fire compartment temperatures. He proposed a simple model of the temperature-time fire development in which only three factors are required: maximum gas temperature, the time at which this maximum temperature occurs, and a shape constant for the curve. Based on a large amount of data correlation [3] using BFD curves he recommended this simple equation can be used to replace international temperature-time curves such as ISO 834, BS 476, ASTM 119, NFPA 251, the external, the hydrocarbon, and the Eurocode parametric curve. Five main advantages of his method compared to other schemes were put forwards in his paper [2]:

\* Corresponding author; e-mail: j0805481@public1.ptt.js.cn

- the BFD curve is a “natural” fire curve that fits the results of actual fire tests closer than previously known fire modeling methods,
- the shape of the curve bears a strong relationship to both the pyrolysis coefficient and the opening factor,
- the shape of the curve is related to the thermal properties of the fire cell,
- contrary to a number of other fire modeling curves, the BFD curve does not need the use of a time shift, and
- it uses a single equation to model the temperature of both the growth and decay phases of a fire in a building whereas a curve such as the Eurocode 1 curve requires two equations.

The research presented in this communication focuses on using the BFD curve to fit the test results of 12 room scale tests in an ISO 9705 compartment. For the two-zone model of the compartment temperature distribution in room fires without flashover, the BFD curve is used to fit the temperature at different spatial points. The errors of the fitted curves are evaluated, with the aim that the test data and the model results may be used amongst the fire safety research community.

### Experimental setup and facilities

Twelve wood crib fire tests were conducted inside an ISO 9705 room, in CSIRO’s Fire Test Laboratory. The hood, exhaust duct, size of room and all instrumentation met the specifications of ISO 9705 [4]. The dimensions of the room are 3.6 m long, 2.4 m wide, and 2.4 m height. There is a single doorway opening to the outside centered on the south wall, as shown in fig. 1, with a width of 0.8 m and height of 2.0 m. The doorway was opened during all room tests. All room tests were conducted with only natural convection driving air ingress into the room. The open factor  $F_{O_2}$  is  $0.05087 \text{ m}^{0.5}$  as calculated by eq. 1:

$$F_{O_2} = \frac{A_v h_v^{0.5}}{A_T} \quad (1)$$

The exhaust gas from the room is collected by a hood outside the doorway. The gas analysis of the exhaust in the duct enabled the heat release from the burning crib to be determined by means of oxygen consumption calorimetry. The instrumentation in the duct met the specifications of ISO 9705. The sampling rate of ISO 9705 is 1 sample per 2.5 seconds.

Three thermocouple trees were used for each test, which were labeled as TC-North, TC-South, and TC-Doorway (fig. 1). Type K MIMS thermocouples (stainless steel sheathed, 1.5 mm diameter) were used on each tree. All trees were composed of 10 thermocouples which were spaced vertically at 200 mm increments, with the lowest thermocouple placed 300 mm from the floor (the uppermost thermocouple being 2100 mm from the floor or 300 mm from the ceiling). The tips of the thermocouples for the tree TC-North was located 100 mm from the north wall and 150 mm from the east wall. These thermocouples have been denoted T<sub>north300</sub>, T<sub>north500</sub>, *etc.* in this manuscript. Thermocouple tree TC-South was located in the south corner of the room with the tip of each thermocouple 100 mm from the south wall and 150 mm from the east wall; the thermocouples are denoted as T<sub>south300</sub> to T<sub>south2100</sub>. All the thermocouples were connected to a data logger.

The nominal heat release rate (HRR) of these cribs was 0.15 MW, 0.25 MW, 0.5 MW, and 1.0 MW. Cribs were put in two positions inside the ISO room, at the center or at the corner. Eight tests

were done on cribs placed at the corner with nominal HRR 0.15 MW, 0.25 MW, 0.5 MW, and 1.0 MW, while 4 tests were conducted on cribs at the centre of the room with the same four nominal HRR.

The wood cribs were made from two sizes of radiata pine wood sticks; dimensions of the sticks were either 35 mm × 35 mm × 500 mm (width × height × length) or 35 mm × 35 mm × 1000 mm. The cribs constructed for 0.15 MW, 0.25 MW, and 0.5 MW HRR only consisted of the shorter sticks. The 0.15 MW, 0.25 MW, and 0.5 MW cribs were composed of 2, 6, and 8 layers of sticks, respectively, with 8 sticks per layer. The 1 MW crib had 12 layers, 6 of which had 16 short sticks per layer and the other 6 layers had 8 long sticks per layer. Sticks had been conditioned at 23 ± 2 °C and 50% ± 5% relative humidity for more than one month before being tested. All the cribs were ignited by spirits in aluminum trays placed underneath the crib. The room environment, nominal fire size, initial mass and positions of these cribs are listed in tab. 1.

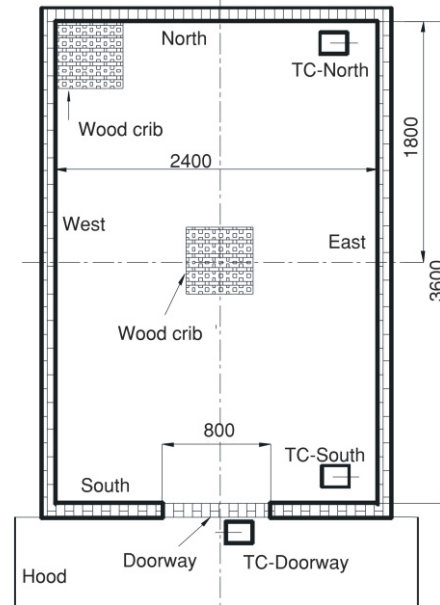


**Figure 1. Test arrangement inside ISO 9705 room**

**Table 1. Cribs and room condition**

| Test label | Position | Nominal fire size [MW] | Initial mass [kg] | Room temp [°C] | Room humidity [%] |
|------------|----------|------------------------|-------------------|----------------|-------------------|
| Test1      | Corner   | 0.150                  | 7.06              | 19.2           | 43.5              |
| Test2      | Corner   | 0.150                  | 7.30              | 18.2           | 53.7              |
| Test3      | Corner   | 0.25                   | 14.06             | 25.1           | 55.3              |
| Test4      | Corner   | 0.25                   | 14.45             | 23.8           | 60.3              |
| Test5      | Corner   | 0.50                   | 30.37             | 21.3           | 45.2              |
| Test6      | Corner   | 0.50                   | 30.15             | 26.2           | 41.5              |
| Test7      | Corner   | 1.0                    | 57.02             | 19.9           | 51.3              |
| Test8      | Corner   | 1.0                    | 58.16             | 22.3           | 46.5              |
| Test9      | Center   | 0.150                  | 7.12              | 18.6           | 53.2              |
| Test10     | Center   | 0.250                  | 14.1              | 18.4           | 46.6              |
| Test11     | Center   | 0.50                   | 29.5              | 17.4           | 47.3              |
| Test12     | Center   | 1.00                   | 54.9              | 17.2           | 46.1              |

## Results and discussion

### Test results

Figure 2. shows the HRR curves for corner fires Test1 to Test8. Test1 and Test2 coincide well to each other, and have HRR peak over the nominal 0.15 MW, nearly 0.2 MW. The HRR peaks of both tests occur earlier than for the larger fires, at nearly 290 second from ignition time. This was attributed to the relatively large porosity factors [5] of these smaller cribs. The transport of air to the centre of these cribs is more rapid, resulting in quick flame spread through the crib. It appears that surface char formation does not impede the wood pyrolysis and significantly restrain combustion. Thus, the HRR curves are not significantly influenced by the char formation and decrease when the volatile component of the fuel is consumed.

For larger cribs, the HRR peaks occur at a later time. This is due to the more compact structure of the cribs. The burning is more significantly influenced by the effect of surface char formation as the porosity factor decreases. The HRR peak of Test3 and Test4 appears around 720 seconds from ignition time, while Test5 has its peak at 770 seconds and Test6 at 810 seconds. The peaks HRR of Test7 and Test8 are later than 900 seconds. Sharp peaks appear on the curves of Test5 and Test7, and this is due to the ignition of paper covering the gypsum panels that lined the room.

Figure 3 illustrates the HRR curves of the centre crib fires Test9 to Test12. As with the corner fires, the delay in reaching the peak HRR with crib size is apparent. Although the HRR reaches 1 MW in Test8, the lower layer temperature is still less than 500 °C. No flashover happened in the 12 tests.

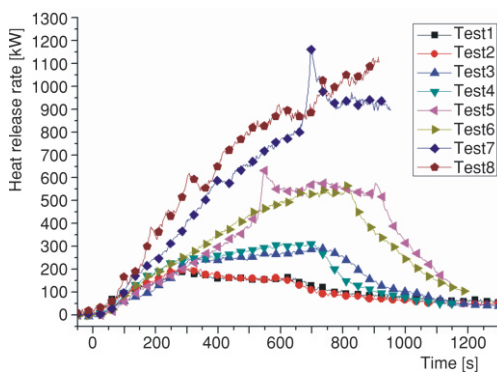


Figure 2. Corner fire HRR

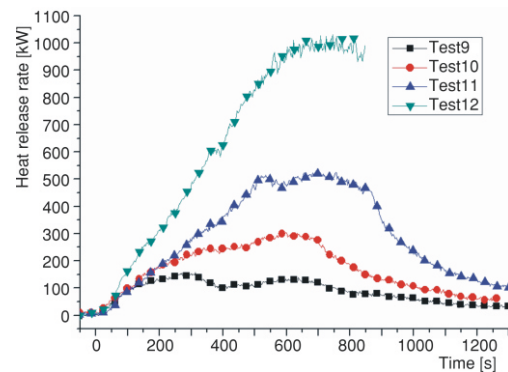


Figure 3. Center fire HRR

Ambient temperatures were subtracted from the measured temperatures. Figures 4 and 5 show the results of TC-North and TC-South in Test2, respectively.

The curves present are typical of what may be expected for a two-zone model of a compartment fire. The interface layer is near  $T_{north1300}$  and  $T_{south1300}$  which is 1300 mm above the floor. The  $T_{north1300}$  and  $T_{south1300}$  fluctuate severely as the flow of cooler incoming air shears against the flow of hotter, out-flowing exhaust gases promoting turbulence between the upper and lower zones. The temperature of the upper zone is significantly higher than

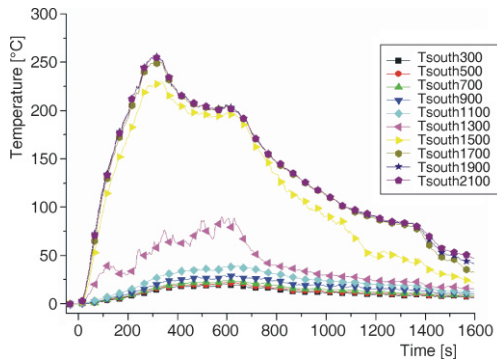


Figure 4. Compartment temperature of TC-South in Test2

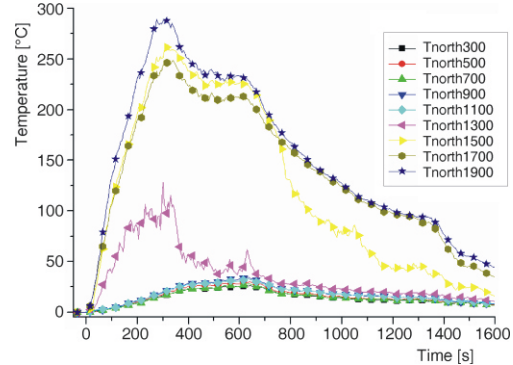


Figure 5. Compartment temperature of TC-North in Test2

that in the lower zone. The shape of the temperature curves in the upper zone mimics that of the HRR curve, not surprisingly as the upper zone temperature is dependent on HRR.

### Modeling of temperature-time curve using the BFD equation

The basic equation that produces a “BFD Curve” is as follows [2]:

$$T = T_a + T_m e^{-z} \quad (2)$$

where  $T$  is the temperature at any time  $t$ ,  $T_a$  – the ambient temperature,  $T_m$  is the maximum temperature generated above  $T_a$ , and

$$z = \frac{(\ln t - \ln t_m)^2}{S_c} \quad (3)$$

where  $\ln$  is the natural logarithm (dimensionless numbers),  $t$  is the time from ignition of fire (Barnett uses minutes, we use seconds in this paper),  $t_m$  – the time at which  $T_m$  occurs, and  $S_c$  – the shape constant for the temperature-time curve (dimensionless numbers). Note that the ambient temperature is subtracted from all the compartment temperatures listed in tab. 1, therefore eq. 4 is substituted for eq. 2. The values of the parameters  $T_m$  and  $t_m$  for thermocouple tree TC-South and TC-North for all 12 tests are listed in tabs. 2 and 3.

$$T = T_m e^{-z} \quad (4)$$

The fitting error  $e_f$  is defined as:

$$e_f = \sqrt{\frac{1}{n(n-1)} \sum_{k=1}^n (T_d(k) - \bar{T}_d)^2} \quad (5)$$

where  $n$  is the total number of samples, and  $T_d$  – the difference between the test temperature  $T$  and the fitted value  $T_f$ , with

$$\bar{T}_d = \frac{1}{n} \sum_{k=1}^n T_d(k) \quad (6)$$

**Table 2.**  $T_m$  and  $t_m$  of TC-south

|        | Tsouth300     |              | Tsouth500     |              | Tsouth700     |              | Tsouth900     |              | Tsouth1100    |              |
|--------|---------------|--------------|---------------|--------------|---------------|--------------|---------------|--------------|---------------|--------------|
|        | $T_m$<br>[°C] | $t_m$<br>[s] |
| Test1  | 17.9          | 575          | 17.1          | 590          | 19.4          | 615          | 20.9          | 640          | 28.5          | 635          |
| Test2  | 20.5          | 590          | 22.2          | 600          | 24.4          | 625          | 29.4          | 630          | 39.3          | 635          |
| Test3  | 39.8          | 805          | 37.5          | 810          | 47.6          | 800          | 54.6          | 800          | 64.1          | 775          |
| Test4  | 49.1          | 745          | 47.3          | 730          | 55.7          | 735          | 63.2          | 755          | 73.1          | 745          |
| Test5  | 117.8         | 895          | 115.7         | 890          | 142.6         | 900          | 155.6         | 910          | 202.9         | 910          |
| Test6  | 129.5         | 795          | 131.4         | 765          | 164.2         | 810          | 170.6         | 810          | 213.7         | 810          |
| Test7  | 322.9         | 1045         | 314.9         | 1045         | 367.4         | 1045         | 411.9         | 1045         | 509.1         | 1045         |
| Test8  | 133.9         | 665          | 135.6         | 665          | 178.6         | 665          | 224.3         | 665          | 261.8         | 660          |
| Test9  | 19.1          | 620          | 22.1          | 630          | 26.9          | 630          | 33.7          | 655          | 104.3         | 595          |
| Test10 | 49.3          | 720          | 57.2          | 705          | 66.7          | 700          | 78.5          | 705          | 110.5         | 700          |
| Test11 | 108.8         | 890          | 122.3         | 880          | 147.6         | 890          | 249.5         | 895          | 351.3         | 890          |
| Test12 | 298.1         | 840          | 322.9         | 840          | 368.2         | 840          | 409.1         | 840          | 499.3         | 840          |
|        | Tsouth1300    |              | Tsouth1500    |              | Tsouth1700    |              | Tsouth1900    |              | Tsouth2100    |              |
|        | $T_m$<br>[°C] | $t_m$<br>[s] |
| Test1  | 81.9          | 445          | 199.2         | 320          | 231.9         | 300          | 239.8         | 295          | 235.6         | 295          |
| Test2  | 89.7          | 580          | 230.5         | 335          | 251.1         | 330          | 256.1         | 320          | 255.3         | 330          |
| Test3  | 78.2          | 800          | 304.7         | 770          | 334.2         | 735          | 339.4         | 730          | 338.3         | 730          |
| Test4  | 87.7          | 740          | 323.4         | 700          | 362.7         | 640          | 366.2         | 640          | 363.9         | 685          |
| Test5  | 347.7         | 910          | 487.4         | 900          | 519.8         | 850          | 530.6         | 850          | 531.1         | 850          |
| Test6  | 313.5         | 805          | 497.7         | 805          | 541.6         | 755          | 546.3         | 735          | 539.5         | 765          |
| Test7  | 648.4         | 1040         | 690.9         | 1040         | 705.1         | 1035         | 713.1         | 1035         | 713.1         | 1035         |
| Test8  | 500.9         | 640          | 567.6         | 640          | 588.1         | 640          | 607.5         | 665          | 597.6         | 665          |
| Test9  | 175.4         | 315          | 188.9         | 305          | 190.5         | 305          | 191.2         | 290          | 192.1         | 295          |
| Test10 | 288.1         | 670          | 317.6         | 635          | 328.7         | 620          | 333.8         | 620          | 330.2         | 620          |
| Test11 | 410.5         | 710          | 508.3         | 785          | 531.3         | 795          | 548.5         | 715          | 550.7         | 730          |
| Test12 | 739.6         | 840          | 788.9         | 840          | 814.4         | 840          | 824.7         | 840          | 821.6         | 840          |

**Table 3.**  $T_m$  and  $t_m$  of TC-North

|        | Tnorth300     |              | Tnorth500     |              | Tnorth700     |              | Tnorth900     |              | Tnorth1100    |              |
|--------|---------------|--------------|---------------|--------------|---------------|--------------|---------------|--------------|---------------|--------------|
|        | $T_m$<br>[°C] | $t_m$<br>[s] |
| Test1  | 24.1          | 615          | 28.5          | 610          | 19.5          | 585          | 29.6          | 580          | 22.7          | 610          |
| Test2  | 26.4          | 650          | 30.2          | 645          | 28.1          | 635          | 34.4          | 635          | 32.9          | 640          |
| Test3  | 58.3          | 755          | –             | –            | –             | –            | –             | –            | 61.7          | 810          |
| Test4  | 64.7          | 710          | 75.1          | 690          | 63.7          | 710          | 80.7          | 720          | 70.1          | 720          |
| Test5  | 142.9         | 900          | 166.4         | 905          | 146.6         | 905          | 171.4         | 910          | 161.8         | 905          |
| Test6  | 163.7         | 805          | 187.2         | 800          | 169.9         | 805          | 196.9         | 805          | 179.9         | 805          |
| Test7  | 357.1         | 1040         | 402.5         | 1045         | 369.8         | 1045         | 411.1         | 1045         | 451.8         | 1050         |
| Test8  | 163.6         | 660          | 201.5         | 650          | 236.6         | 650          | 236.2         | 650          | 226.1         | 650          |
| Test9  | 14.8          | 670          | 16.6          | 670          | 18.3          | 660          | 23.1          | 660          | 107.5         | 555          |
| Test10 | 40.9          | 695          | 45.3          | 700          | 45.1          | 690          | 56.4          | 690          | 66.5          | 700          |
| Test11 | 94.1          | 885          | 110.9         | 890          | 119.4         | 885          | 142.3         | 885          | 278.2         | 895          |
| Test12 | 299.3         | 880          | 360.4         | 880          | 384.1         | 880          | 533.1         | 880          | 610.3         | 880          |
|        | Tnorth1300    |              | Tnorth1500    |              | Tnorth1700    |              | Tnorth1900    |              | Tnorth2100    |              |
|        | $T_m$<br>[°C] | $t_m$<br>[s] |
| Test1  | 117.2         | 265          | 184.5         | 300          | 216.4         | 295          | 254.7         | 290          | –             | –            |
| Test2  | 128.1         | 305          | 261.2         | 315          | 249.2         | 345          | 289.2         | 280          | 266.7         | 280          |
| Test3  | 73.5          | 755          | 356.4         | 725          | 361.7         | 750          | 416.1         | 725          | 453.8         | 740          |
| Test4  | 82.4          | 705          | 342.8         | 600          | 428.2         | 685          | 464.1         | 690          | 504.2         | 675          |
| Test5  | 283.7         | 970          | 569.5         | 910          | 672.3         | 865          | 731.8         | 805          | 807.6         | 820          |
| Test6  | 277.3         | 925          | 598.2         | 810          | 683.6         | 785          | 745.5         | 780          | 808.6         | 755          |
| Test7  | 687.3         | 1050         | 899.1         | 1040         | 935.5         | 1035         | 956.2         | 1035         | 966.1         | 1045         |
| Test8  | 545.8         | 630          | 689.4         | 640          | 732.6         | 625          | 779.2         | 565          | –             | –            |
| Test9  | 167.7         | 310          | 174.2         | 305          | 176.6         | 305          | 176.6         | 305          | 123.4         | 305          |
| Test10 | 280.2         | 645          | 294.6         | 645          | 297.2         | 645          | 297.7         | 645          | 227.4         | 640          |
| Test11 | 361.8         | 885          | 446.2         | 740          | 466.4         | 745          | 477.2         | 740          | 389.2         | 740          |
| Test12 | 687.3         | 840          | 708.9         | 840          | 727.9         | 800          | 743.1         | 800          | 647           | 800          |

According to Barnett's study [2],  $S_c$  is calculated based on following equations:

– for uninsulated fire compartments

$$S_c = \frac{1}{4.00F_{O_2} - 0.10} \quad (7)$$

– for insulated fire compartments

$$S_c = \frac{1}{9.25F_{O_2} - 0.21} \quad (8)$$

For the ISO 9705 room,  $S_c$  is 3.30 for an uninsulated room and 1.47 for an insulated room. But these values are not appropriate to all tests. The typical value of  $S_c$  calculated by recommended equations does not fit the data very well, but the fit can be improved by varying this constant.

Equation 4 is used to fit the compartment temperatures. Figure 6 is the model result for two temperature curves in the upper zone, while fig.7 shows the two results for the lower zone,

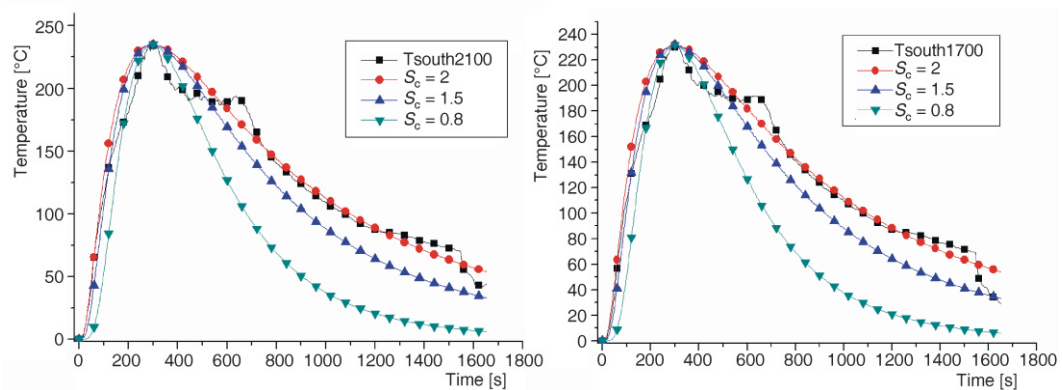


Figure 6. Fitting of upper zone temperature

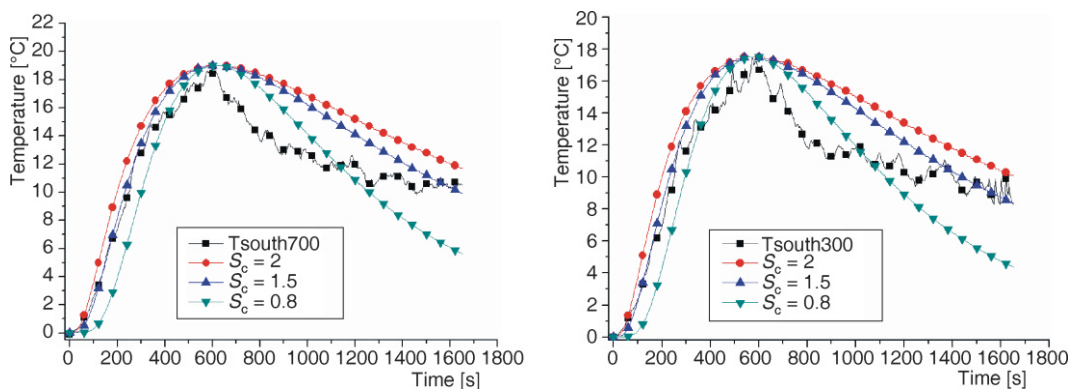


Figure 7. Fitting of lower zone temperature

all for the TC-South thermocouple tree. It can be seen that the value of  $S_c$  that gives the better fit to the experimental data differs depending on whether the thermocouple is placed in the hotter upper zone or the cooler lower zone. The model curve with  $S_c = 2$  gives the best fit to the measured temperature for the upper zone. The agreement between model data and experimental data is much closer for temperatures in the upper zone than for those in lower zone. This was also true for the results are obtained for TC-North.

The fitting error ( $e_f$ ) is calculated for different shape constant ( $S_c$ ). A typical result is shown in fig. 8. The value of  $e_f$  varies from 0.04 to 0.06 for  $S_c$  values of 1.5 to 3 for upper zone curves (Tsouth1500 to Tsouth2100). This implies the fact that the values of  $S_c$  that give the best fit lie between the values calculated for insulated and uninsulated rooms. The large fluctuations in the temperature measured at Tsouth1300, which is placed near the interface between the upper and lower zones, results in a large value of  $e_f$  regardless of the value of  $S_c$ . For the lower zone, the range of  $S_c$  that provides the best fit is from 1.8 to 3.2 with  $e_f$  from 0.07 to 0.09.

Figure 9 illustrates the minimum fitting error with corresponding shape constant for TC-South fittings in all tests. Test1, Test8, and Test12 have the lowest fitting errors, while Test5, Test7, and Test11 have the largest errors. The error depends on the original shape of temperature curves. Test5 and Test7 have abnormal peaks caused by burning of cover paper.

Figure 11 illustrates the minimum fitting error with corresponding shape constant for TC-North fittings in all tests. Test1, Test8, and Test12 have the

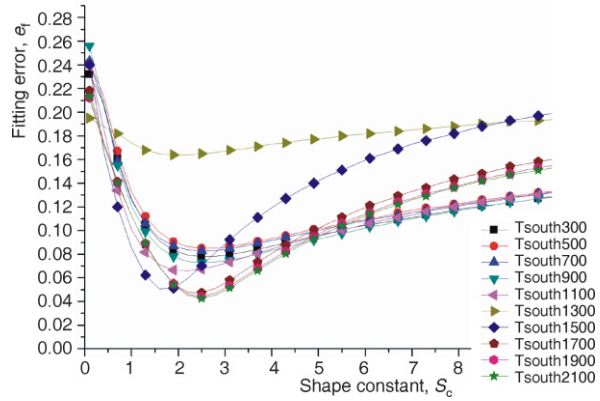


Figure 8. Fitting errors with different  $S_c$

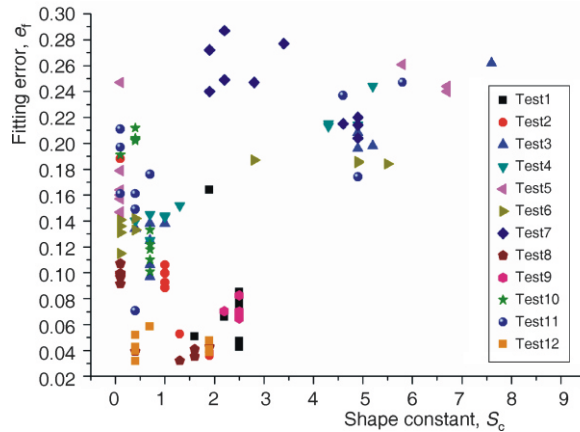


Figure 9. The minimum fitting error with the thermocouple position for TC-South in all test

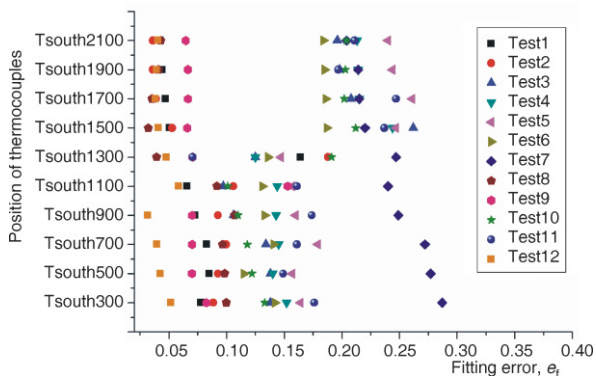


Figure 10. The minimum fitting error of fitting for TC-South

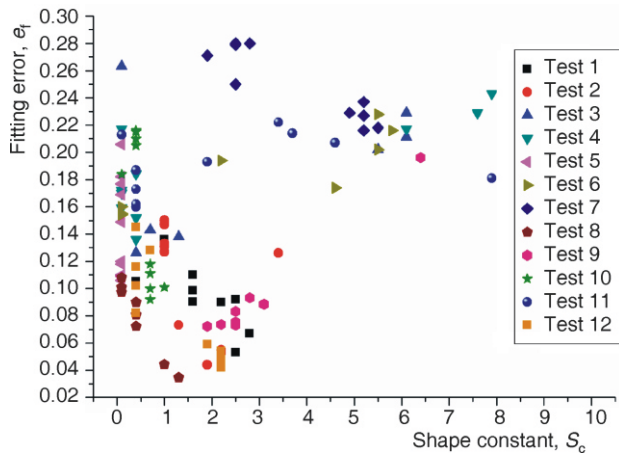


Figure 11. The relationship of minimum fitting error and  $S_c$  in fitting of TC-North

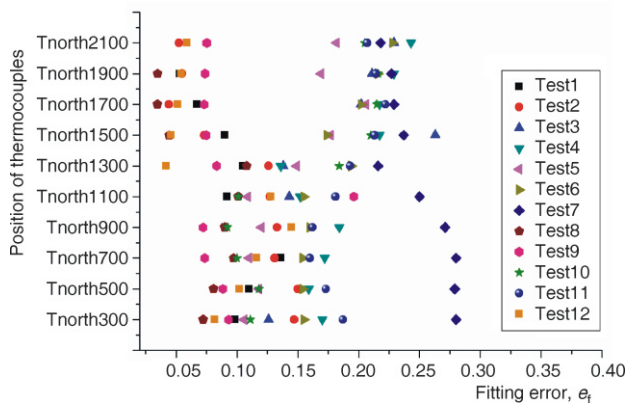


Figure 12. The minimum fitting error of fitting for TC-North

lowest fitting errors (which is same as those in TC-South – refer fig. 9), while Test7 and Test11 have the largest errors.

Figure 12 illustrates the minimum fitting errors for TC-North in all tests. It shows similar results as given in fig. 10. The overall error in the lower zone is less than that in upper zone, and the errors are grouped between 0.05 and 0.20, except for Test7. The 1300 mm level is an interface level for both TC-South and TC-North. Above this level the error is separated into two groups with fitting error from 0.03 to 0.07 (Test1, Test2, Test8, Test9, and Test12) and from 0.17 to 0.27 (Test3, Test4, Test5, Test6, Test7, Test10, and Test11). This does not appear to be any relationship between the position of the cribs or fire size as to what grouping the data is placed.

## Conclusion

The temperature-time data for a crib fire in an ISO 9705 size room were modeled using a BFD curve. A good fit between experimental and model data could only be obtained when the constant  $S_c$  could be varied, *i. e.* it could not be predicted accurately from the equation given in the model. The shape of the predicted curve seemed to fit the temperature in the upper zone of the room more accurately than in the lower zone of the room. Clearly, more research is needed for the temperature distribution in the room to be predicted with such simple models. Sharing the fire test data-base resource in the fire safety research community would be helpful towards meeting this goal.

## Acknowledgments

The research is supported by the Natural Science Fund of China, No. 50876045. This research also used the facilities established from Natural Science Fund of Jiangsu Province, No. BK2008416 and financial support from State Key Laboratory of Fire Science, No. HZ2007-KF11.

## Nomenclature

|           |   |       |  |
|-----------|---|-------|--|
| $A_F$     | – floor area of the compartment, [m <sup>2</sup> ]                                  | $S_c$ | – shape constant for the temperature-time curve, [–]                         |
| $A_T$     | – internal surface area less opening, [m <sup>2</sup> ]                             | $T$   | – temperature at any time, [°C]  |
| $A_v$     | – sum of areas of vertical openings, [m <sup>2</sup> ]                              | $T_a$ | – ambient temperature, [°C]  |
| $e_f$     | – fitting error based on dimensionless temperature $T_d/T_m$ , [–]                  | $T_d$ | – difference between test temperature and fitting value (= $T - T_f$ ), [°C] |
| $F_{O_2}$ | – opening factor based on $A_F = A_v h_v^{0.5}$ , [m <sup>0.5</sup> ]               | $T_f$ | – fitting temperature at any time, [°C]                                      |
| $F_v$     | – ventilation factor of vertical openings (= $A_v h_v^{0.5}$ ), [m <sup>2.5</sup> ] | $T_m$ | – maximum temperature generated above $T_a$ , [°C]                           |
| $h_v$     | – weighted mean height of vertical openings, [m]                                    | $t$   | – time from ignition of fire, [s]  |
| $Q$       | – energy output from fire, [kW]   | $t_m$ | – time at which $T_m$ occurs, [s]  |

## References

- [1] \*\*\*, The SFPE Handbook of Fire Protection Engineering, 3<sup>rd</sup> ed., ISBN: 087765-451-4
- [2] Barnett, C. R., BFD Curve: a New Empirical Model for Fire Compartment Temperatures, *Fire Safety Journal*, 37 (2002), 5, pp. 437-463
- [3] Barnett, C. R., Replacing International Temperature-Time Curves with BFD Curve, *Fire Safety Journal*, 42 (2007), 4, pp. 321-327
- [4] \*\*\*, ISO 9705 Fire Tests Full-Scale Room Test for Surface Products, International Organization for Standardization, Geneva, 1993
- [5] Gross, D., Res, J., National Bureau of Standards, C. Engineering Instrumentation, 66C (1962), 2, pp. 99-105